Dispersion-mode pulsed laser

Baruch Fischer, Boris Vodonos, Shimie Atkins, and Alexander Bekker

Department of Electrical Engineering, Technion–Israel Institute of Technology, Haifa 32000, Israel

Received January 5, 2000

A new self-consistency condition in pulsed lasers with strong intracavity dispersion imposes dispersion modes with specific cavity-length dependent pulse rates, utilizing pulse-train self-imaging properties of a temporal Talbot effect. We give an experimental demonstration of such a laser operation, using a long fiber cavity. We also demonstrate temporal Talbot imaging of a train of short pulses that propagate along large distances of dispersive fibers. © 2000 Optical Society of America

OCIS codes: 140.3510, 070.6760, 060.5530, 260.2030.

Light pulses that propagate along dispersive media change their shapes and spread in a way similar to how spatially confined waves, such as Gaussian beams, diffract and spread as they propagate in free space. Therefore, if we wish to construct an amplitude-modulated laser that has strong accumulated dispersion in its cavity, pulse oscillation will generally be problematic because the pulses do not reproduce themselves after one or more round trips in the cavity. This difficulty can cause very lossy and complex pulse operation. Thus, for example, mode-locked operation of a long fiber laser, with significant dispersion, is not likely to produce good-quality short pulse trains. In this Letter we show that operation of such lasers is possible in a specific regime in which a pulse train is self-imaged after a certain propagation distance. The pulse-train self-imaging property is related to the spatial Talbot effect,[1] in which periodic spatial patterns that propagate in free space are self-reproduced at specific distances that are multiples of the Talbot length. Accordingly, we show that the self-consistency condition dictates specific values for the laser round-trip cavity length, which are multiples of half the Talbot length. For a given cavity length, the self-consistency condition defines a series of allowed values for the pulse rate. These values can be regarded as dispersion resonances or dispersion modes (D-modes) of a temporal Talbot laser. Here we present experimental demonstrations of such a laser operation. We also give an experimental demonstration of reproduction of trains of short pulses that propagate in long distances of dispersive fibers. This method can be used to transmit very short pulse trains through long distances of dispersive fibers.

The explanation of the time-domain Talbot effect, which is the basis for the present work, is similar to the known spatial Talbot effect.[1] As for beam diffraction in free space, the propagation of pulses in a dispersive medium in the slowly varying amplitude approximation is described by a Schrödinger-like equation,[2,3]

$$i\,\frac{\partial \psi}{\partial z} = \frac{\beta_2}{2}\,\frac{\partial^2 \psi}{\partial \tau^2}\,. \tag{1}$$

Here the propagation is along z, and $\tau = t - z/v_g = t - \beta_1 z$ is the internal pulse-time variable (relative to the center of the pulse), where $v_g = 1/\beta_1$ is the group velocity and β_2 is the group-velocity dispersion (responsible for pulse broadening). We have neglected third- and higher-order dispersion terms.

It is straightforward to see that a field envelope of an input periodic pulse train $\psi(\tau, z = 0)$, with a rate or pulse-train frequency $f = \Omega/2\pi$, reproduces itself as it propagates at distances that are multiples of the so-called Talbot length[1] $z_T = 4\pi/(\beta_2 \Omega^2)$. First, we express the field envelope as a Fourier series:

$$\psi(\tau, z = 0) = \sum_n a_n \exp(in\Omega\tau)\,. \tag{2}$$

Then, the propagation in the dispersive medium adds to each component in the series the quadratically n-dependent phase factor $\exp(i\gamma n^2/2)$, where[3] $\gamma = \beta_2 z \Omega^2$, giving at a distance z

$$\psi(\tau, z) = \sum_n a_n \exp(in\Omega\tau)\exp(i\gamma n^2/2)\,. \tag{3}$$

Therefore, when $\gamma/2 = 2\pi m$ (m is an integer), which occurs for $z = m z_T = 4\pi m/(\beta_2 \Omega^2)$, we have

$$\psi(\tau, z = m z_T) = \psi(\tau, z = 0)\,, \tag{4}$$

an exact reproduction of the original pulse train. At half-Talbot distances (odd multiples of $z_T/2$), where $\gamma/2 = (2m + 1)\pi$, we have

$$\psi[\tau, z = (2m + 1)(z_T/2)] = \psi[\tau + (\pi/\Omega), z = 0]\,, \tag{5}$$

or the periodic pulse train is shifted by half a period. At other distances the pulse-train shape and rate are modified. For example, for $z_T/4$, the rate is doubled.

We have demonstrated temporal Talbot self-imaging of pulse trains in a dispersive fiber. Figure 1 gives the experimental results, showing the input and the self-imaged pulse train that has propagated 50 km in the fiber.

We return to the dispersive pulsed laser. It can have a linear or a ring configuration. The self-consistency condition for its operation is that the pulse train is reproduced after one round trip between successive amplitude modulations. This happens for cavity round-trip lengths that are multiples of z_T. Nevertheless, multiples of half of the Talbot distance are sufficient for that requirement, since the π phase shift of the reproduced pulse train can be compensated for by propagation at half a period. Therefore the self-consistency requirement for the dispersion-embedded

0146-9592/00/100728-03$15.00/0

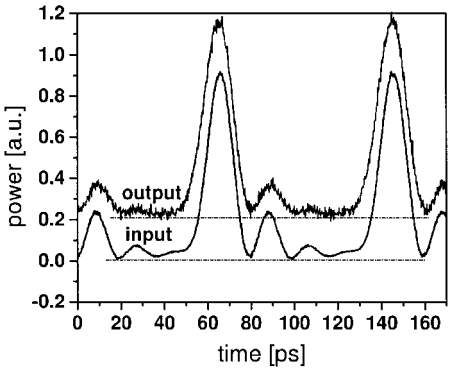

Fig. 1. Talbot imaging of a pulse train in a dispersive fiber, showing the original pulse train and its reproduction at half the Talbot distance, with $L = z_T/2 = 50$ km, corresponding to $\beta_2 = -20.7$ ps^2/km and $\Omega = 12.4$ GHz. The amplitudes of the signals are normalized, and for clarity the zero level is shifted and marked by dotted–dashed lines. The ripple following each pulse is probably an artifact that is due to the detector.

pulsed laser that the round-trip cavity length be $L_m = mz_T/2$ or that the pulse rate be

$$\Omega_m{}^2 = 2\pi m/(\beta_2 L). \tag{6}$$

Equation (6) determines the D-modes. Other cavity lengths may allow operation of the laser, especially for multiples of other rational numbers and fractions of the Talbot length (where pulses can be retrieved after several cycles), but more-complex pulse structures, as well as higher losses and higher laser thresholds, are expected.

An additional requirement for operation of such a laser is synchronization, such that the pulse train perfectly reaches the successive modulations after each round trip in the cavity. This condition is met when $f = \Omega/2\pi = sv_g/L$, where s is an integer. This means that the pulse rate equals an s harmonic of the cavity mode, or that the laser is mode locked. Thus, for a proper operation of a dispersive pulsed laser, the modulation frequency has to match both a D-mode resonance frequency and a harmonic of the regular mode-locking cavity resonance frequency. For real operating conditions we performed the following calculation: Typical values of the first D-mode in a laser with a standard fiber at wavelengths of ~1550 nm, and with a group-velocity dispersion of $\beta_2 \approx -20$ ps^2/km, are $L = z_T/2 \approx 50$ km and $f = 12.62$ GHz. On the other hand, for such long cavities, the basic regular cavity resonance frequency for mode locking is only $f = v_g/L \approx 4$ kHz. Therefore, very high-order harmonics, of the order of $s \sim 10^5$–10^6, are needed for the mode-locking frequency to reach the ~10-GHz pulse-rate regime.

The experimentally studied laser configuration is shown in Fig. 2. It is a ring cavity consisting of a long fiber, an erbium-doped fiber amplifier pumped by a 980-nm diode laser, and a $LiNbO_3$ amplitude modulator. We used two types of fiber: The first was a regular fiber with anomalous dispersion of $\beta_2 \approx -19.4$ ps^2/km, for $\lambda = 1530$ nm and length $L = 50$ km, with the first D-mode resonance at $f_1 = 12.8$ GHz. We also used a fiber with a positive, high group-velocity dispersion, $\beta_2 \approx +132$ ps^2/km, for $\lambda = 1531$ nm, which permitted the use of shorter lasers. Here the cavity length that we used was $L = 5.1$ km, and the pulse rate for the first D mode was $f_1 = 15.4$ GHz. This fiber with the positive group-velocity dispersion also ensured that no solitons formed during pulsed laser operation.

The output of the experimental lasers, the pulse trains, and the spectra are shown in Figs. 3–6. The resolution of the spectrum analyzer was 15 pm. The minimum measured pulse widths were ~15 ps, close to the limit of the oscilloscope and the photodetector, which had a 50-GHz bandwidth. We also measured the width of the pulses by use of the second-harmonic generation autocorrelation technique and obtained a similar result [see inset of Fig. 4(a)]. We can see the different behaviors of laser operation when the frequencies are tuned to the first D-mode resonances or away from resonances. At resonance, we obtain high-quality pulses with a broad Gaussian spectrum. Away from resonance, the pulses are almost diminished or have a complex structure. The spectra have more-complex shapes and are generally

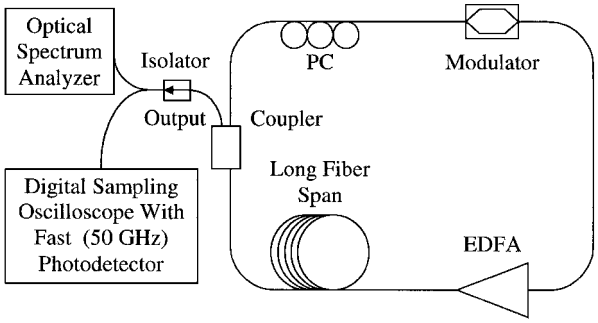

Fig. 2. Experimental configurations of the pulsed lasers, consisting of a fiber ring cavity with an erbium-doped fiber amplifier (EDFA) and a $LiNbO_3$ amplitude modulator. PC, polarization controller.

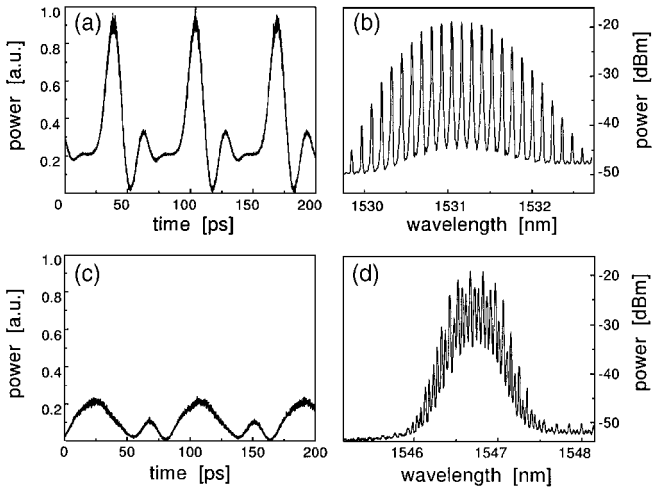

Fig. 3. Output spectrum and signal from the laser with $\beta_2 = 132$ ps^2/km, $L = 5.1$ km: operation (a) and (b) at the first D-mode resonance ($f = 15.4$ GHz) and (c) and (d) out of resonance ($f = 12.0$ GHz). The same scale is used for (a) and (c).

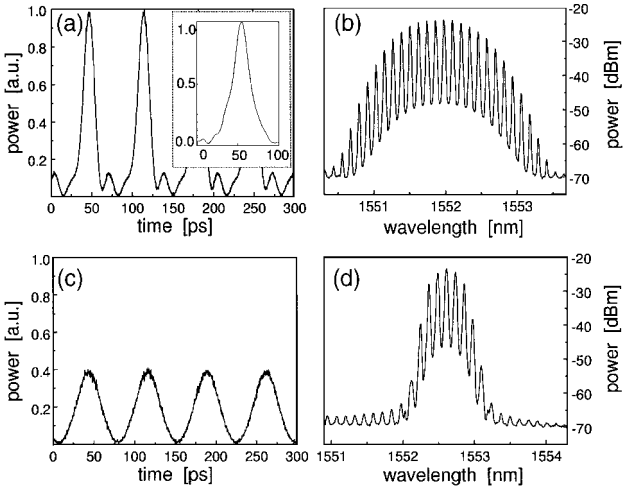

Fig. 4. Same as in Fig. 3 but for a different bias condition, modulation frequency, and lasing wavelength: operation near resonance, with $f = 14.8$ GHz, and out of resonance, with $f = 13.8$ GHz. Temporal autocorrelation of pulses obtained by use of second-harmonic generation is shown in the inset of (a).

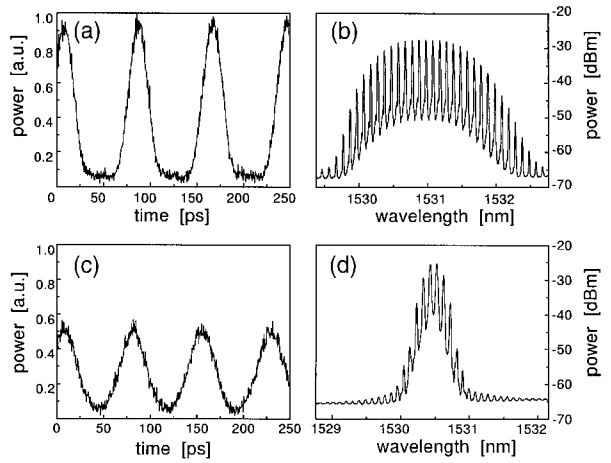

Fig. 5. Output spectrum and signal from the laser with $\beta_2 = -19.4$ ps^2/km, $L = 50$ km: operation (a) and (b) at the first D-mode resonance ($f = 12.8$ GHz) and (c) and (d) out of resonance ($f = 13.8$ GHz). The same scale is used for (a) and (c).

more confined. At resonance, matching the D-mode requirement is equivalent to the case in which the dispersion effect and the propagation shrink to zero.[4] Then, the successive modulations of the light pulses in the cavity after each round-trip propagation increase the sideband number and give broad Gaussian spectra. Away from the D-mode resonance, round-trip propagation between two successive modulations adds arbitrary phases to the frequency components of the pulse train in Eq. (3). These phases can cause confinement of the spectrum, as can be seen in Figs. 3–6, and, at special regimes, can also result in a more-specific localization effect that limits sideband formation in the frequency domain.[3] This mechanism limits short-pulse formation in such mode-locked lasers. The confined spectrum, when localization occurs, in some regimes has an exponential envelope,

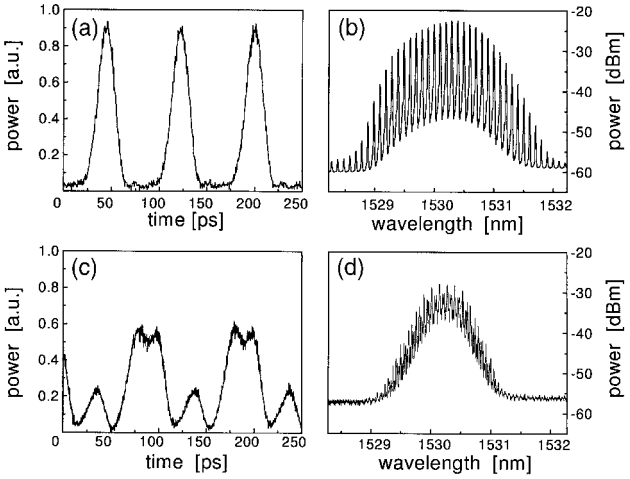

Fig. 6. Same as in Fig. 5 but for different bias conditions: operation near resonance, with $f = 12.8$ GHz, and out of resonance, with $f = 10.0$ GHz.

whereas the spectrum has a broad Gaussian shape at D-mode resonance operation. This can be seen in the experimental spectra in Figs. 3–6.

It is also important to note that, when the applied modulation frequency is slightly shifted, the laser can self-adjust to the D-mode condition by a change in the lasing wavelength as a result of the β_2 dependence on the wavelength. This flexibility permits the different lasing wavelengths in Figs. 3 and 4. In addition, a change of the bias of the $LiNbO_3$ modulator affects the signal and the spectrum's modulation depth but does not alter their basic features.

In conclusion, we have shown the requirements for the operation of pulsed lasers with high intracavity dispersion. The self-consistency condition dictates specific values for the pulse-rate square (or for the product of the pulse-rate square and the total dispersion). A demonstration was performed with a pulsed laser with a long fiber cavity.

This work was partially supported by the Consortium for Broadband Communication, administered by the Chief Scientist of the Israel Ministry of Commerce and Industry, and by the Division for Research Funds of the Israel Ministry of Science, the Israel Ministry of Commerce and Industry, and the Fund for Promotion of Research at the Technion. B. Fischer's e-mail address is fischer@ee.technion.ac.il.

References

1. L. Liu, Appl. Opt. **28,** 4668 (1989); **49,** 833 (1982).
2. G. P. Agrawal, *Nonlinear Fiber Optics*, 2nd ed. (Academic, San Diego, Calif., 1995).
3. B. Fischer, A. Rosen, and S. Fishman, Opt. Lett. **21,** 1463 (1999).
4. B. Fischer, A. Rosen, A. Bekker, and S. Fishman, "Experimental observation of localization in the spatial frequency domain of a kicked optical system," Phys. Rev. E (to be published); A. Rosen, B. Fischer, A. Bekker, and S. Fishman, "Optical kicked system exhibiting localization in the spatial frequency domain," J. Opt. Soc. Am. B (to be published).